1 Effect of host species on the topography of fitness landscape

2 for a plant RNA virus

- 3
- 4
- 5 Héctor Cervera,^a Jasna Lalić,^{a,#} Santiago F. Elena^{a,b,c*}
- 6

7 Instituto de Biología Molecular y Celular de Plantas (IBMCP), Consejo Superior de
8 Investigaciones Científicas-Universidad Politécnica de Valencia, València, Spain^a;
9 Instituto de Biología Integrativa y de Sistemas, Consejo Superior de Investigaciones
10 Científicas-Universitat de València, Valencia, Spain^b; The Santa Fe Institute, Santa Fe,
11 New Mexico, USA^c

- 12
- 13 Running Head: empirical fitness landscapes
- 14

15 [#]Present address: Jasna Lalić, Division of Molecular Biology, Institute Ruđer Bošković,

- 16 Zagreb, Croatia
- 17 *Address correspondence to sfelena@ibmcp.upv.es
- 18 H.C. and J.L. contributed equally to this work.
- 19

Journal of Virology

Accepted Manuscript Posted Online

20 ABSTRACT

21 Adaptive fitness landscapes are a fundamental concept in evolutionary biology that 22 relate the genotype of individuals with their fitness. At the end, the evolutionary 23 fate of evolving populations depends on the topography of the landscape, that is, 24 the number of accessible mutational pathways and of possible fitness peaks (i.e, 25 adaptive solutions). For long time, fitness landscapes were only theoretical constructions due to a lack of precise information on the mapping between 26 27 genotypes and phenotypes. In recent years, however, efforts have been devoted to 28 characterize the properties of empirical fitness landscapes for individual proteins 29 or for microbes adapting to artificial environments. In a previous study, we had 30 characterized the properties of the empirical fitness landscape defined by the first 31 five mutations fixed during adaptation of tobacco etch potyvirus (TEV) to a new 32 experimental host, Arabidopsis thaliana. Here we evaluate the topography of this 33 landscape in the ancestral host Nicotiana tabacum. Comparing the topographies of 34 the landscape in the two hosts, we found that some features remain similar, such as the existence of fitness holes and the prevalence of epistasis, including cases of sign 35 and of reciprocal sign that create rugged, uncorrelated and highly random 36 37 topographies. However, we also observed significant differences in the fine-38 grained details among both landscapes due to changes in the fitness and epistatic 39 interactions of some genotypes. Our results support the idea that not only fitness 40 tradeoffs between hosts but also topographical incongruences among fitness 41 landscapes in alternative hosts may contribute to virus specialization.

42

43 IMPORTANCE

Journal of Virology

45 is known about the topography of virus adaptive fitness landscapes and even less is 46 known about the effect that different host species and environmental conditions 47 may have of this topography. To bring this gap, we have evaluated the topography 48 of a small fitness landscape formed by all genotypes that result from every possible 49 combination of the five mutations fixed during adaptation of TEV to its novel host 50 A. thaliana. To assess the effect that host species may have on this topography, we 51 evaluated the fitness of every genotype both in the ancestral and novel hosts. We 52 found both landscapes share some macroscopic properties such as the existence of 53 holes and being highly rugged and uncorrelated, yet they differ in microscopic 54 details due to changes in the magnitude and sign of fitness and epistatic effects.

Despite its importance for understanding virus' evolutionary dynamics, very little

55

44

The effect of mutations can be influenced by their interactions with other mutations, 56 57 with the environment or both. Epistatic interactions among genetic loci determine the 58 ruggedness of fitness landscapes. In the absence of epistasis, landscapes are single-59 peaked and smooth (1). For such simple landscapes, predicting the result of evolution is 60 an easy task. By contrast, epistatic interactions create curvature in the landscape and, if being of the sign or reciprocal sign types, they create multiple peaks separated by low 61 fitness valleys (1 - 3). The reproducibility of evolution, and therefore our ability to 62 63 predict its outcome, in such complex landscapes diminishes as the number of possible peaks, that is the ruggedness of the landscape, increases. Therefore, epistasis strongly 64 65 determines the pace, reproducibility and predictability of adaptive walks on fitness landscapes. 66

67 Mutations do not only interact among them in determining fitness; mutations also interact with the external environment, making the phenotypes plastic (4, 5). In 68 69 practical terms, in the case of viruses the environment mostly reduces to the host, 70 although environmental factors such as temperature, or the presence of other coinfecting 71 viruses or cellular pathogens may affect the replication of viruses as well. Not all 72 potential hosts in the host range (different species or genotypes from the same species) 73 of a virus are equally susceptible to infection, and it is generally assumed that a tight 74 matching may exist between host-genotypes and virus-genotypes to allow a virus to 75 successfully infect a host (6). Indeed, substantial amount of data supports the idea that 76 by evolving into a single host species or genotype viruses become specialists (7 - 10) 77 whereas by evolving in multiple host species, the result may be no-cost generalists (7, 78 11 - 13).

Downloaded from http://jvi.asm.org/ on September 1, 2016 by NORTHERN ILLINOIS UNIV

Furthermore, epistasis and phenotypic plasticity mutually interact in a very intricate
 manner (14 - 16). The evolutionary consequences of these interactions are important.

81 For example, by changing the pattern of epistasis it is possible to access mutational 82 pathways that may be maladaptive in one environment but not so in another (17 - 20). 83 Understanding the roles that environmental changes and landscape topology have in the 84 number and nature of adaptive pathways would allow predicting the potential avenues 85 of future evolution. Despite this importance, how environmental heterogeneity affects 86 the topography of fitness landscapes is still poorly understood, and only few recent 87 studies have started to tackled this problem; mostly in the context of the evolution of antibiotic resistances (20 - 23) or during experimental adaptation of Escherichia coli to 88 89 an artificial glucose-limited environment (24).

90 The aim of the present study is to explore the effect of environmental changes on 91 the topography of an empirical fitness landscape in a biologically relevant context: an RNA virus and its eukaryotic multicellular hosts. Previously, we constructed the 2^5 = 92 93 32 genotypes that comprise all possible combinations of the first five mutations (Table 94 1) fixed by Tobacco etch virus (TEV; genus Potyvirus, family Potyviridae) during 95 experimental evolution on a novel host, A. thaliana (25). In this previous work, we 96 evaluated the topography of this fitness landscape in the novel host (26), showing it was 97 rugged and with holes created by the existence of lethal genotype. We also showed that 98 higher-order epistasis, that is, interactions between more than pairs of mutations 99 contributed in a significant manner to the architecture of fitness (26). Here we follow 100 up with this study by evaluating the fitness of all the 32 genotypes in the ancestral host, 101 N. tabacum. Comparing both fitness landscapes, we found that some features remain 102 similar among hosts, such as the existence of lethal genotypes and the prevalence of 103 epistasis that create a highly rugged topography. However, we also observed significant 104 differences in the fine grained details among both landscapes due to host-specific 105 effects both in fitness and epistasis.

106

107 MATERIALS AND METHODS

108 Generation of viral genotypes. All 32 TEV mutant genotypes used in this study were 109 constructed by successive rounds of site-directed mutagenesis starting from the template plasmid pMTEV that contains a full copy of the genome of a wildtype TEV isolated 110 111 from tobacco (GenBank accession DQ986288) (27), using mutagenic primers with specific single-nucleotide mismatches (26) and Phusion[®] High-Fidelity DNA 112 Polymerase (Finnzymes). PCR mutagenesis profile consisted of 30 s denaturation at 98 113 114 °C, followed by 30 cycles of 10 s at 98 °C, 30 s at 60 °C, and 3 min at 72 °C, ending 115 with 10 min elongation at 72 °C. Next, the PCR-mutagenesis products were incubated 116 with DpnI (Fermentas) for 2 h at 37 °C to digest the methylated parental DNA template. 117 E. coli DH5 α electrocompetent cells were transformed with 2 μ l of these reactions 118 products and plated out on LB agar supplemented with 100 µg/ml ampicillin. Bacterial 119 colonies were inoculated in 8 ml LB-ampicillin liquid medium and grown for 16 h in an orbital shaker (37 °C, 225 rpm). Plasmid preparations were done using Pure YieldTM 120 121 Plasmid Maxiprep System (Promega) and following the manufacturer's instructions. 122 Incorporation of mutation was confirmed by sequencing a ca. 800 bp fragment 123 circumventing the mutagenized nucleotide. The plasmid DNA was BglII linearized and in vitro transcribed using mMESSAGE mMACHINE® SP6 Kit (Ambion) in order to 124 125 obtain infectious RNA of each virus genotype (28).

Plants inoculation. *N. tabacum* L. cv. Xanthi *NN* plants were used for production of a large stock of virus particles from each of the 32 genotypes. Batches of eight-week old *N. tabacum* plants were inoculated with 5 μg of RNA of each viral genotype by abrasion of the third true leaf. Ten days post-inoculation (dpi), the whole infected plants were collected and pooled for each virus genotype. Next, plant tissue was frozen with liquid N₂, homogenized using mortar and pestle and aliquoted in 1.5 ml tubes.
Saps were prepared by adding 1 ml of 50 mM potassium phosphate buffer (pH 8.0) per
gram of homogenized plant tissue, centrifuged at 4 °C and 10000 g for 10 min and the
upper liquid phase taken and mixed with 10% Carborundum (w/v).

These stocks were used to mechanically inoculate either between 3 and 31 (median 12) *A. thaliana* L. ecotype L*er*-0 plants, at growth stage 3.5 according to Boyes scale (29), or 6 4-weeks old *N. tabacum* plants. Plants were maintained in a Biosafety Level-2 greenhouse at 25 °C and 16 h light period. Infection status was determined by one step RT-PCR after 21 dpi for *A. thaliana*.

Lethal genotypes and failed experiments produce the same result: a lack of infection. To deal with this possible source of error, we proceeded as described elsewhere (5, 26, 28). In short, we estimated the probability of failing an inoculation experiment using RNA transcripts from wildtype pMTEV using a large number of plants. Then, using this probability, we applied the Bernoulli probability distribution to evaluate the likelihood of failing all inoculation experiments after a given number of trials. In all cases, this probability was < 0.01. Downloaded from http://jvi.asm.org/ on September 1, 2016 by NORTHERN ILLINOIS UNIV

147 Virus genomic RNA purification and quantification of viral load. RNA 148 extraction from 100 mg of tissue per plant was performed using Agilent Plant RNA 149 Mini Kit (Agilent Technologies) following manufacturer's instructions. The 150 concentration of total plant RNA extracts was adjusted to 100 ng/µl for each sample and 151 the quantification of viral load was done with absolute real time RT-qPCR using 152 standard curves (30). Standard curves were constructed using 10 serial dilutions of 153 TEV genome produced as described above and diluted in total plant RNA obtained from 154 healthy tobacco or arabidopsis plants, treated like all other plants in the experiment. Quantification amplifications were done in 20 µl volume using an ABI StepOnePlusTM 155

Real-Time PCR System (Applied Biosystems) with the GoTaq[®] 1-sStep RT-qPCR 156 System (Promega) as follows: RT phase consisted of 15 min at 37 °C and 10 min at 95 157 °C; PCR phase consisted of 40 cycles of 10 s at 95 °C, 34 s at 60 °C and 30 s at 72 °C; 158 159 final phase consisted of 15 s at 95 °C, 1 min at 60 °C and 15 s at 95 °C. Amplifications 160 were performed in 96-well plates, each plate containing the RNA samples necessary to 161 build the corresponding standard curve; quantifications were performed in triplicate for 162 each sample in different plaques. Quantification results were examined using StepOne 163 software v. 2.2.2 (Applied Biosystems)

164 Fitness determinations and statistical analyses. Total RNA was extracted and 165 virus accumulation was quantified by RT-qPCR as described above and detailed in (30). 166 Virus accumulation (pg of TEV RNA per 100 ng of total plant RNA) was quantified at t 167 = 21 dpi for A. thaliana infected plants and t = 5 for N. tabacum infected plants to 168 ensure viral populations were at exponential growth in both cases (TEV reaches a quasi-169 stationary plateau faster in N. tabacum than in A. thaliana). These values were then 170 used to compute the fitness of the mutant genotypes relative to the wildtype genotype on each host species using the expression $W = \sqrt[t]{R_t/R_0}$, where R_0 and R_t are the ratios 171 172 of accumulations estimated for the mutant and reference viruses, respectively, at 173 inoculation and after t days of growth (28).

174 A generalized linear model (GLM) was fitted to the fitness data. The model 175 incorporated three random factors: host species (H), virus genotype (G) and plant (P), 176 which represents the unit of biological replication (different individual plants from host 177 species H infected with viral genotype G). H and G were considered as orthogonal 178 factors whereas P was nested within the interaction of the H and G. The model 179 equation reads:

180
$$W_{ijkl} = \mu + G_i + H_j + (G \times H)_{ij} + P(G \times H)_{ijk} + \xi_{ijkl},$$
 Eq. 1

181 where μ is the grand mean value and ξ_{ijkl} is the error associated with individual measure 182 l (estimated from the technical replicates of the RT-qPCR reactions). The statistical 183 significance of each factor was evaluated using a likelihood ratio test (LRT) that asymptotically follows a χ^2 distribution. The magnitude of effects was evaluated using 184 the η_P^2 statistic, the ratio of variance explained by the effect while controlling for the 185 other effects. Effects with $\eta_P^2 \ge 0.25$ are considered as large. Variance components 186 187 were estimated by maximum likelihood. Statistical analyses were performed with IBM 188 SPSS software version 23.

189 Representation of fitness landscapes. A simple way to represent fitness 190 landscapes is in the form of a graph where each node corresponds to a specific 191 genotype. Instead of representing genotypes in terms of nucleotides or amino acids, one 192 can only indicate whether wildtype or mutant alleles are present at a given site, *i.e.* the 193 possible entries at each site are either \bigcirc or \bullet , respectively, giving rise to a binary graph. 194 With this notation, wildtype TEV is represented as 00000 while the Arabidopsis-195 adapted isolate is represented as •••••. Edges in the binary graph represent 196 mutational steps of size one, that is, connecting genotypes that only differ in one allele.

Downloaded from http://jvi.asm.org/ on September 1, 2016 by NORTHERN ILLINOIS UNIV

197 Evaluation of landscapes ruggedness. The ruggedness of the landscape on the 198 two hosts was evaluated using three different approaches: (i) the mean slope to 199 roughness ratio, $\theta(31)$, (ii) the correlation between neighbor's fitness, ρ , (32) and (iii) 200 the frequency of different types of epistatic interactions. θ measures how much the 201 slope of a given peak spikes out from the average surface in which it exists. A value of 202 $\theta >> 1$ means that a peak emerges from an otherwise flat surface, similar to a Mount 203 Fuji landscape; by contrast, a value of $\theta \leq 1$ would indicate that the peak's slope does 204 not differ substantially from the background surface, that is, it is surrounded by many 205 small peaks of similar slope (31). ρ measures the similarity between the fitness of Journal of Virology

 \geq

lournal of Virology

206 genotypes that occupy nearby positions in the landscape. If this correlation is perfect ($\rho \approx 1$), then the landscape is absolutely smooth; as epistasis becomes more and more 208 prevalent, then this correlation is reduced, and $\rho < 0$ for the case of sign and reciprocal 209 sign epistasis (Fig. 1) (32).

210 In terms of their effect on landscape topography, four different types of epistatic 211 interactions can be defined (Fig. 1). If magnitude epistasis exists, the fitness of the 212 double mutant is different from the multiplicative expectation (see below for a 213 mathematical definition of this condition). In the example shown in Fig. 1b, the 214 observed fitness of the double mutant is larger than expected (positive epistasis); in the 215 cases of no epistasis (Fig. 1a) or of magnitude epistasis (Fig. 1b), the effects of both 216 mutations are unconditionally beneficial. If the effect of one of the mutations is 217 conditionally beneficial (i.e., beneficial in one genetic background but deleterious in 218 another), then we are in the situation of sign epistasis (Fig. 1c). Finally, if both 219 mutations are deleterious by themselves, but beneficial when combined, we are in the 220 situation of reciprocal sign epistasis (Fig. 1d). The more common the cases of sign and 221 reciprocal sign epistasis, the more rugged the landscape.

The graphical representation of the two landscapes and the estimation of the above parameters describing their topography were obtained using the MAGELLAN webserver (33).

225 **Computation of epistasis.** The magnitude of epistasis among mutations *i* and *j* 226 was calculated as $\varepsilon_{ij} = W_{00}W_{ij} - W_{i0}W_{0j}$, where W_{i0} and W_{0j} are the relative fitnesses 227 of genotypes carrying each single mutation, W_{ij} is the relative fitness of the double 228 mutant, W_{00} is the fitness of the wildtype (34, 35). The second term on the right-hand 229 side of the equation corresponds to the expected fitness which, under the hypothesis of 230 multiplicative independent effects, equals the observed fitness, resulting in $\varepsilon_{ij} = 0$. 231 Deviations from the null hypothesis indicate antagonistic ($\varepsilon_{ij} > 0$) and synergistic ($\varepsilon_{ij} <$ 232 0) epistasis, respectively. For genotypes containing more than two mutations, a very similar equation can be used: $\varepsilon_{i(k)} = W_{00}W_{i(k)} - W_iW_{(k)}$ but in this case $W_{(k)}$ 233 234 corresponds to the fitness of the genotype containing k mutations into which mutation i235 has been introduced and $\varepsilon_{i(k)}$ is the epistasis between mutation i and the genetic 236 background containing the k other mutations. For example, genotype $\bullet \circ \bullet \bullet \circ$ could 237 be constructed in three ways: inserting mutation $\bigcirc \bigcirc \bigcirc \bigcirc \bigcirc \bigcirc \bigcirc$ into genetic background 238 $\bullet \circ \bullet \circ \circ$, inserting mutation $\circ \circ \bullet \circ \circ$ into genetic background $\bullet \circ \circ \circ \circ \circ$, and by 239 inserting mutation •0000 into 00••0, meaning that we can test for three cases of 240 epistasis in this genotype. This decomposition of interactions generates 75 possible 241 genetic combinations for which epistasis was tested. Following the mathematical 242 conditions given in (36), we evaluated whether those cases for which we estimated a 243 significant epistasis coefficient also corresponded to sign or reciprocal sign epistasis.

244 Higher-order epistasis were also evaluated using the Walsh coefficients, as 245 proposed in (37), using the MAGELLAN webserver (33). Walsh coefficients have their 246 equivalent in classic population genetics (37): (i) zero-order Walsh coefficients 247 represent the mean fitness across all genotypes; (ii) first-order Walsh coefficients are 248 equivalent to the selection coefficients, which represent the fitness effects of single 249 mutations; (iii) second-order Walsh coefficients are equivalent to pairwise epistatic 250 coefficients, ε_{ii} ; and (iv) higher-order Walsh coefficients are thus equivalent to higher-251 order epistatic interactions among the > 2 mutations present in a genotype. In the case 252 of multiplicative fitness landscapes, all Walsh coefficients for order ≥ 2 are equal to 253 zero and, thus, the landscape is smooth. In contrast, ruggedness is maximal in a fully 254 random landscape, with many local peaks representing all types of epistatic interactions, 255 and thus, the mean squared epistatic coefficients increase exponentially with order.

256 Real fitness landscapes shall lie between these two extremes, neither smooth nor 257 maximally rugged (37).

258

259 RESULTS

260 Landscapes topographies and first descriptive statistics. Fig. 2 shows both 261 estimated landscapes and Table 2 contains some statistics describing their topographies. 262 Defining a peak as a genotype such that all their neighbors have lower fitness, in A. 263 *thaliana*, these 32 genotypes define a landscape with two peaks (genotypes $\bigcirc \bigcirc \bigcirc \bigcirc$ 264 and $\bigcirc \bigcirc \bullet \odot \bigcirc \bigcirc$ of different height (26), whereas four peaks are defined in the ancestral 265 host N. tabacum (genotypes $\bigcirc \bigcirc \bigcirc \bigcirc , \bigcirc \bigcirc \bigcirc \bigcirc , \bigcirc \bigcirc \bigcirc \bigcirc , and \bigcirc \bigcirc \bigcirc \bigcirc$. The 266 ruggedness of the landscape can be evaluated using several different measures (Table 267 2). For instance, the ratio between mean slope and roughness, θ , (31) took similar 268 values for both hosts, and in both cases values were greater than 1, indicating that the 269 landscapes are rugged in relationship to the average slope of the peaks. The amount and 270 type of epistasis also describe the topography of a landscape. A recently proposed 271 measure of epistasis is the correlation between fitness effects of a given genotype and 272 all their one-step neighbors, ρ (32). In our case, both ρ values are positive and small, 273 close to zero, suggesting the existence of many cases of magnitude epistasis. Another 274 very intuitive measure of the ruggedness of a landscape is to compute the frequency of 275 each type of epistatic interactions among all possible pairs of mutations, for a smooth 276 landscape, the fraction of multiplicative interactions should be maximal; as the 277 ruggedness of the landscape increases, cases of sign and of reciprocal sign epistasis 278 should become more common (2, 36). Table 2 indicates that most mutations interacted 279 epistatically in both hosts, with magnitude epistasis being the most common type of 280 interaction in both landscapes. Sign epistasis was the second most common type of 281 epistasis in *A. thaliana* while reciprocal sign epistasis was so for the ancestral host *N. tabacum*. All together, these result suggest that the landscape defined by these five
283 mutations is more rugged in the ancestral host than in the new one. We will further
284 expand these results in the next sections.

285 Fitness correlations and antagonistic pleiotropy among hosts. To further 286 explore the relationship between the topographies of both landscape shown in Fig. 2, we 287 have evaluated the similarity in the fitness effects estimated for each genotype in each 288 host species (Fig. 3a). Fitness values are significantly correlated among the two 289 landscapes (Pearson's r = 0.891, 30 d.f., P < 0.001). However, this correlation is 290 entirely driven by the existence of a group of genotypes that are lethal in both hosts. If 291 these genotypes are removed from the analysis the correlation is not significant 292 anymore (r = 0.338, 20 d.f., P = 0.124). The dashed lines in Fig. 3a represent the 293 relative fitness of the wildtype TEV in both hosts. These lines divide the fitness space 294 in four regions, each region corresponding to the genotypes with fitness values greater 295 or smaller than the wildtype $(\bigcirc \bigcirc \bigcirc \bigcirc \bigcirc)$ in each hosts. Twelve genotypes had fitness 296 values greater than wildtype in both hosts and thus are unconditionally beneficial. By 297 contrast, 10 genotypes were unconditionally deleterious, with fitness values smaller 298 than wildtype in both hosts. Nine of them were lethal in both hosts and genotype 299 00000 was lethal in A. thaliana but only slightly deleterious (-0.5% effect) in N. 300 tabacum. Together, these 22 genotypes occupying the upper-right and lower-left 301 quadrants of Fig. 3a account for the above correlation. Cases in the other two quadrants 302 are more interesting as they represent examples of antagonistic pleiotropy: genotypes 303 beneficial in one host that are deleterious in the alternative one. Genotype ●0000 304 was beneficial in N. tabacum but it was deleterious in A. thaliana. Eight genotypes had 305 fitness values greater than the wildtype in A. thaliana but were deleterious in the

original host. Given their low fitness in the ancestral host, most likely these genotypeswere generated and selected during the process of adaptation to the new host.

308 Prior to any further statistical analyses, fitness data were checked for violation of 309 the assumptions of normality and homocedasticity of variances. We found that data 310 were not normally distributed (one-sample Kolmogorov-Smirnov test: D = 0.248, P < 0.2480.001) nor variances were homogeneous among groups (Levene test: $F_{229,399} = 13.980$, 311 312 P < 0.001). The GLM described in Eq. 1, with a gamma distribution and a log-link 313 function (chosen because it had the minimal Bayes information criterion among a set of 314 alternatives tested), was fitted to the fitness data to evaluate the relative contribution of 315 genotypes and host species to the observed variability in fitness. Table 3 shows the 316 results of this analysis. Overall, highly significant differences exist among the 32 317 genotypes (P < 0.001), which largely contribute to the observed differences in fitness 318 $(\eta_P^2 = 0.860)$. The percentage of total variance explained by true genetic differences 319 among viral genotypes is as large as 77.8%. The net contribution of host species to 320 viral fitness is also significant (P = 0.037), although the magnitude of the effect is very small ($\eta_P^2 = 0.006$; variance explained by host: only 0.2%) and consequently the 321 322 statistical power associated to this test is too low to make the result reliable. However, 323 a highly significant effect (P < 0.001) of host species that depends on each genotype exists, being the magnitude of this interaction effect also large ($\eta_P^2 = 0.500$; variance 324 325 explained by interaction: 16.7%). The fact that the interaction between viral genotypes 326 and host species contributes to fitness in a much larger extent than host species itself has 327 an important consequence: the two landscapes differ in fine-grained details more than 328 they do in the coarse-grained details. Finally, differences among plants of each host 329 species inoculated with the same viral genotype are also significant (P < 0.001) and of a

magnitude comparable to that of the main virus effect ($\eta_P^2 = 0.848$), but explains a relatively minor fraction of the total observed variance (4.2%).

332 Differences in epistasis and landscape ruggedness among hosts. Next, we 333 explored the congruency between epistasis values and types across host species for all 334 genotypes carrying two or more mutations. Computing epistasis between pairs of 335 mutations is straightforward, however, for genotypes carrying more than two mutations, the computation becomes slightly more complicated. For example, for a triple mutant, 336 337 we must consider the three different cases in which each single mutation is introduced 338 into the corresponding complementary double-mutant genotypes (see Materials and 339 Methods for an example). By doing so, we have to analyze a total of 75 different 340 possibilities (26). Fig. 3b shows these data and illustrates the existence of a significant correlation between epistasis coefficients measured in both hosts (r = 0.718, 73 d.f., P <341 342 0.001). However, a substantial number of interactions do not fit the diagonal expected 343 under the hypothesis of no host effect on epistasis. Most of these cases, 10, had 344 negative epistasis in N. tabacum that changed into multiplicative effects or even positive 345 epistasis in A. thaliana.

346 Genetic interactions in A. thaliana can be classified as follows: 40 cases are 347 multiplicative, 26 of magnitude epistasis, four of sign epistasis, and five of reciprocal 348 sign epistasis (26) (Table 4). In N. tabacum the counts per category are: 46 cases of 349 multiplicative interactions, 11 of magnitude epistasis, seven of sign epistasis, and 11 of 350 reciprocal sign epistasis. The distribution of counts per categories is significantly different among hosts ($\chi^2 = 10.050$, 3 d.f., P = 0.018), with an excess of cases of sign 351 352 and reciprocal sign in N. tabacum. The epistasis-transition matrix (Table 4) shows the 353 effect that experimental adaptation to A. thaliana had on the different types of epistasis. 354 Most of the interactions remained of the same type on both hosts (65.3%, Binomial test

Accepted Manuscript Posted Online

Journal of Virology

Σ

355 P = 0.011), mainly due to the congruency in the number of multiplicative cases. 356 Interestingly, among those that changed the type of epistasis, 57.5% did so in the 357 direction of reducing the ruggedness of the landscape (*e.g.*, from sign or reciprocal sign 358 to magnitude) in *A. thaliana*.

359 Seeking for a mechanistic understanding of these changes in the patterns of 360 epistasis, we will focus in pairwise interactions due to their simplicity. Five 361 combinations of two mutations resulted in a reduction of the landscape's ruggedness in 362 A. thaliana compared to N. tabacum, in three cases from reciprocal sign epistasis to 363 magnitude epistasis and in one case from sign epistasis to multiplicative effects. 364 Noteworthy, four out of these five case involved synonymous mutation P1/U357C 365 $(\bigcirc \bigcirc \bigcirc \bigcirc \bigcirc \bigcirc$). No obvious explanation can be brought forward to explain why the effect 366 of a synonymous mutation depends so strongly on the presence of mutations in other 367 genes. Another interesting case is nonsynonymous mutations $6K1/T1126M (\bigcirc \bigcirc \bigcirc \bigcirc$). 368 The 6K1 small peptide is required for viral replication and colocalizes with chloroplast-369 bounded viral replicase elements 6K2 and NIb at early stages of infection (38). The 370 fitness effects resulting from the interaction between this particular mutation at 6K1 and 371 all other four mutations were always host-dependent. When combined with 372 synonymous mutation P1/U357C or with nonsynonymous mutation P3/A999V 373 374 magnitude epistasis in A. thaliana, respectively. However, when this mutation was 375 combined with nonsynonymous mutation VPg/L1965F ($\bigcirc \bigcirc \bigcirc \bigcirc \bigcirc$) or with synonymous 376 mutation NIaPro/C6906U (0000), it increased ruggedness from multiplicative to 377 sign or to magnitude epistasis, respectively, in the novel host. Again, no obvious 378 mechanism can be brought forward to explain why the effect of this mutation depends 379 on synonymous mutations in other genes. The fitness effect of 6K1/T1126M is 380 alleviated in presence of mutation P3/A999V in the novel host, suggesting some form of 381 interaction between these two genes (either direct or indirect) not yet detected 382 experimentally (39). The beneficial fitness effect of 6K1/T1126M is potentiated in 383 presence of mutation VPg/L1965F in the novel host, also suggesting that these two 384 proteins may tightly coordinated actions in determining TEV fitness in the novel host. 385 Neither a direct interaction between these two proteins has been confirmed 386 experimentally (39). However, in both cases, an indirect interaction mediated by the CI 387 protein may still be possible (39).

388 So far, we have focused on pairwise interactions between individual mutations or 389 between a mutation and a group of them. Weinreich et al. (37) pointed out that this 390 approach must be misleading as the products of many genes interact in complex 391 manners to determine the fitness of individuals, thus higher-order epistasis must be a 392 fundamental component of the genetic architecture of fitness. Using the Walsh's 393 coefficients approach proposed in (37), we have evaluated the contribution of higher-394 order epistasis to the two landscapes. Fig. 4 compares the weight of each Walsh's 395 coefficient to the fitness variability observed in both landscapes. The zero-order 396 coefficients represent the mean fitness across all genotypes. In this case, mean fitness is 397 higher in the novel host than in the ancestral one. This is logical, since these genotypes, 398 at least those that may have a real existence in the evolving population, were positively 399 selected in A. thaliana. First-order coefficients correspond to selection coefficients of 400 single mutations. In both landscapes, up to four-order interactions contribute in a 401 noticeable manner to the observed pattern of fitness, illustrating the complexity of 402 interactions between genes in determining TEV fitness in both hosts. Interestingly, 403 second-order interactions, that correspond to pairwise epistasis coefficients, seem to be 404 qualitatively more important in A. thaliana, while third-order interactions representing

405 the effect of a given mutation on the curvature of the surface defined by two other 406 mutations (i.e., second-order interactions) appear to be more important in N. tabacum. 407 The different weight of second- and third-order interactions in each hosts further 408 supports the idea that the landscape was less rugged in the novel host than in the 409 ancestral one. Four-order interactions also appear to be qualitatively more important in 410 A. thaliana than in N. tabacum. Four-order coefficients reflect the effect that a surface 411 defined by a pair of mutations exerts on the surface defined by another pair of 412 mutations. Unfortunately, we cannot provide and intuitive visualization this numerical 413 result.

414 Relationship between antagonistic pleiotropy and the sign of epistatic 415 interactions. Pleiotropy and epistasis have strong parallelisms because the effect of an 416 allele depends on the context in both cases: the host species for pleiotropy and the virus' 417 genetic background for epistasis. Indeed, it has been postulated that pleiotropy is a 418 prerequisite for epistasis (3, 40). This dependence is obvious for the case of sign 419 pleiotropy, where mutations with a positive effect in the new host have a negative effect 420 in the primary one (13). Furthermore, in the context of compensatory evolution, 421 antagonistic pleiotropy is a precondition for sign epistasis, because it allows for the 422 negative pleiotropic effects of previously selected mutations to be compensated by 423 additional ones (3). Therefore, it is of interest to test whether the eight genotypes 424 showing evidences of antagonistic pleiotropy (see comments above on Fig. 3a), all of 425 them carrying nonsynonymous mutations 6K1/T1126M, also change the sign of their 426 epistatic interactions in both hosts. Indeed, all eight genotypes show a change in the 427 sign of their epistatic interactions: genotype OOOO from negative to positive and the 428 other seven genotypes from positive to negative. By contrast, among the 18 genotypes 429 not showing evidences of antagonistic pleiotropy, 14 do not change the sign of their

430 epistatic interactions among hosts species and four do change (three from negative to 431 positive and only one from positive to negative). A Fisher's exact test confirms that changes in the sign of epistasis are significantly enriched among genotypes showing 432 433 antagonistic pleiotropy compared with genotypes that did not showed it (P < 0.001).

434

435 DISCUSSION

436 The results described above clearly illustrate that changes in host species result in 437 perturbations in the topography of the fitness landscape of an RNA virus. The five 438 mutations fixed during experimental evolution of TEV in the novel host A. thaliana, 439 conformed a landscape in the original host, N. tabacum, that was significantly more 440 rugged that the landscape in the novel host. Differences among both landscapes, 441 however, were local rather than global, with particular genotypes changing their relative 442 height in the landscape and resulting in different patterns of epistatic interactions with 443 their neighbors. This dependence of the topography of the fitness landscape on the host 444 supports the notion of dynamic landscapes (17) or seascapes (19) rather than of static 445 ones. Nonetheless, both landscapes shared common features, such as the existence of 446 fitness holes due to unconditionally lethal genotypes or the presence of pervasive 447 epistatic interactions. The topography of both empirical landscapes match pretty well 448 with the expectations from a random uncorrelated landscape; lying somewhere between 449 the extreme case of the House-of-Cards model (31, 41), in which the fitness of each 450 genotype is absolutely independent on the fitness of the other genotypes, and the less 451 radical case of the rough Mount Fuji model (31, 42), which combines properties of both 452 the House-of-Cards and of a purely multiplicative landscape.

453 Antagonistic pleiotropic fitness effects have been widely reported for RNA viruses 454 adapting to different hosts and are generally accepted as the main cause of fitness 455 tradeoffs among hosts that drive virus specialization to novel hosts (reviewed in (43)). 456 Here we have found that ~26% of genotypes have a pleiotropic fitness effect, with all 457 but one of these cases corresponding to genotypes beneficial in the novel host but 458 deleterious in the ancestral one. These results further stress the importance of 459 antagonistic pleiotropy in driving adaptation to local new host at the cost of a reduced 460 fitness in the ancestral one. Other authors, however, consider that fitness tradeoffs have 461 been overrated as the mechanism explaining virus' host specialization (44, 45). Indeed, 462 it has been proposed that incongruent fitness landscapes may be a better explanation for 463 the evolution of specialist viruses infecting alternative hosts (45). Our results show that 464 these two hypotheses can be conciliated: some genotypes represent clear examples of 465 antagonistic pleiotropy while both landscapes are incongruent in some particular details. 466 Indeed, both hypotheses are not mutually exclusive as antagonistic pleiotropy largely 467 contributes to the incongruence among landscapes.

468 We have also found that antagonistic pleiotropy in host usage and epistasis at the 469 genomic level go hand by hand, thus corresponding to a situation defined as epistatic 470 pleiotropy (13). Indeed, we have previously reported a similar result when analyzed the 471 fitness and epistatic interactions of a larger collection of random mutations on TEV 472 genome (16). Epistatic pleiotropy has two important implications. Firstly, unlike either 473 sign or magnitude pleiotropy in the absence of epistasis, epistatic pleiotropy allows for 474 the evolution of either specialist or no-cost generalist viruses, depending on the virus 475 population's host. Secondly, and very important to limit the emergence of new viruses, 476 when epistasis is in the form of reciprocal sign epistasis, the ruggedness of the adaptive 477 landscapes diminishes the ability of viral populations to escape from specialism to a 478 situation of no-cost generalism. A long history of evolution in the primary host may 479 result in an adaptive walk towards a host-specific fitness peak involving most, if not all,

viral loci. Such a population could find itself many mutational steps away fromreaching a generalist peak.

482 In recent years evolutionary biologists have started to tackle the topography of 483 fitness landscapes from an empirical perspective (reviewed in (1)). Unfortunately, the 484 amount of information about fitness landscapes is still very limited. Empirical fitness 485 landscapes have been thoroughly explored only for another virus, HIV-1, for mutations 486 allowing access to alternative cell surface chemokine co-receptor (46 - 48), and for 487 adaptation to different antiviral drugs (49). In both cases, ruggedness has been proved 488 to be common due to the pervasiveness of epistasis. In the latter case, results suggested 489 that the coarse-grained details of the topography were only weakly dependent on 490 environmental conditions, in this case the presence of different antiretroviral drugs (49). 491 Our results are in good agreement with these previous findings.

492 How can viral population reach the global fitness maximum in such a highly rugged 493 landscape and not be trapped in suboptimal fitness peaks? Here we have shown that by 494 changing the host species the landscape has been flattened off, facilitating the access to 495 certain peaks that otherwise may remain inaccessible in the ancestral host. There are 496 other possible mechanisms for efficiently improving fitness in such landscapes that do 497 not necessarily require moving one step at a time. This long-range jumps are known as 498 stochastic tunneling in large populations (50). Recombination is the most obvious 499 mechanism for such tunneling effect as it may combine beneficial mutations into a 500 single genotype. At least for TEV, the recombination rate is on the same ball park than 501 mutation rate (51) and high recombination rates are not rare among (+)ssRNA viruses 502 (52). The typically high mutation rates of RNA viruses, usually on the vicinity of one 503 per genome and replication round (53), combined with their very fast replication rates 504 and large population sizes make likely that a double mutant carrying two beneficial

lournal of Virology

505 mutations could be created, thus allowing for the tunneling effect. In the case of TEV, 506 genomic mutation rate is U = 0.601 (54). Assuming that only a very minor fraction of 507 all possible individual mutations is beneficial, say only one per genome, the lower 508 bound probability of finding a genome carrying two of such beneficial mutations would be $U_b^2 = (0.601/9539)^2 = 3.97 \cdot 10^{-9}$. From an evolutionary perspective the number that 509 matters is the product NU_b^2 , where N is the population census size. This product gives 510 511 the number of individuals in the population that are double mutants. For TEV N512 strongly varies among hosts but in the case of susceptible A. thaliana ecotypes, it is always greater than 10^8 and it can be as large as 10^{10} genomes per plant (55), thus 513 making NU_b^2 very likely to be greater than one during the course of most infections. 514

515 Some readers may consider as caveats of this study that (i) A. thaliana is not a 516 natural host of TEV and (ii) that all our experiments have been performed in controlled 517 greenhouse conditions that may be optimal for virus replication and accumulation. We 518 do not consider the first to be a real problem as this study, and all previous ones 519 performed with the same experimental pathosystem (25, 26, 30, 55 - 59), deal with the 520 evolutionary determinants and consequences of viral emergence and adaptation to a 521 fully novel host. The second may certainly be an issue to be considered. It is well 522 known that A. thaliana, and wild hosts in general, support less replication than crops or 523 hosts grown in greenhouse conditions (60). In this sense, our arguments above for 524 efficient landscape exploration based on stochastic tunneling may not work well in the 525 wild if replication levels are reduced. Therefore, generalizing our findings and 526 conclusions to a natural ecological context may not be straightforward... as it might be 527 the case for almost every experimental evolution study, at least, if not for every 528 laboratory experiment.

As a closing consideration, gathering information on the structure and topology of RNA virus' adaptive landscapes, on their dependence on external factor and on how they modulate virus evolution may be central for developing new antiviral strategies, personalized clinical treatments and predicting and containing emerging diseases of viral etiology.

534

535 ACKNOWLEDGEMENTS

536 We thank Francisca de la Iglesia and Paula Agudo for technical assistance. We thank537 Dr. J.A. Daròs for kindly providing plasmid pMTEV.

538

539 FUNDING INFORMATION

540 This project was funded by grants BFU2012-30805 and BFU2015-65037P from the 541 of Spanish Ministry Competitiveness (MINECO), Economy and 542 PROMETEOII/2014/021 from Generalitat Valenciana and EvoEvo (ICT610427) from 543 the European Commission 7th Framework Program to S.F.E. H.C. was supported by 544 contract BES2013-065595 from MINECO. J.L. was supported by a JAE-pre contract 545 from CSIC.

546

547 REFERENCES

- De Visser JAGM, Krug J. 2014. Empirical fitness landscapes and the
 predictability of evolution. Nat Rev Genet 15:480-490.
- Weinreich DM, Watson RA, Chao L. 2005. Sign epistasis and genetic constraint
 on evolutionary trajectories. Evolution 59:1165-1174.
- De Visser JAGM, Cooper TF, Elena SF. 2011. The causes of epistasis. Proc R
 Soc B 278:3617-3624.

Journal of Virology

Journal of Virology

554

4.

Remold SK, Lenski RE. 2001. Contribution of individual random mutations to 555 genotype-by-environment interactions in Escherichia coli. Proc Natl Acad Sci USA 556 **98**:11388-11393. 557 5. Lalić J, Cuevas JM, Elena SF. 2011. Effect of host species on the distribution of 558 mutational fitness effects for an RNA virus. PLoS Genet 7:e1002378. 559 Agrawal AF, Lively CM. 2003. Modelling infection as a two-step process 6. 560 combining gene-for-gene and matching-allele genetics. Proc R Soc B 270:323-334. 561 7. Turner PE, Elena SF. 2000. Cost of host radiation in an RNA virus. Genetics 562 156:1465-1470. 563 8. Duffy S, Turner PE, Burch CL. 2006. Pleiotropic costs of niche expansion in the 564 RNA bacteriophage \$6. Genetics 172:751-757. 565 9. Agudelo-Romero P, de la Iglesia F, Elena SF. 2008. The pleiotropic cost of host-566 specialization in tobacco etch potyvirus. Infect Genet Evol 8:806-814. 10. Bedhomme S, Lafforgue G, Elena SF. 2012. Multihost experimental evolution of 567 568 a plant RNA virus reveals local adaptation and host-specific mutation. Mol Biol 569 Evol 29:1481-1492. 11. Remold SK, Rambaut A, Turner PE. 2008. Evolutionary genomics of host 570 571 adaptation in Vesicular stomatitis virus. Mol Biol Evol 25:1138-1147. 572 12. Coffey LL, Vignuzzi M. 2011. Host alternation of Chikungunya virus increases 573 fitness while restricting population diversity and adaptability to novel selective 574 pressures. J Virol 85:1025-1035. 575 13. Remold SK. 2012. Understanding specialism when the Jack of all trades can be the 576 master of all. Proc R Soc B 279:4861-4869. 577 14. Remold SK, Lenski RE. 2004. Pervasive joint influence of epistasis and plasticity 578 on mutational effects in Escherichia coli. Nat Genet 36:423-426.

- 579 15. Lalić J, Elena SF. 2012. Epistasis between mutations is host-dependent for an
- 580 RNA virus. Biol Lett **9**:20120396.
- 581 16. Elena SF, Lalić J. 2013. Plant RNA virus fitness predictability: contribution of
- 582 genetic and environmental factors. Plant Pathol **62**:S10-S18.
- 17. Laughlin DC, Messier J. 2015. Fitness of multidimensional phenotypes in
 dynamic adaptive landscapes. Trends Ecol Evol 30:487-496.
- 18. Matuszewski S, Hermisson J, Kopp M. 2014. Fisher's geometric model with a
 moving optimum. Evolution 68:2571-2588.
- 19. Mustonen V, Lässig M. 2009. From fitness landscapes to seascapes: non equilibrium dynamics of selection and adaptation. Trends Genet 25:111-119.
- 589 20. Steinberg B, Ostermeier M. 2016. Environmental changes bridge evolutionary
 590 valleys. Sci Adv 2:e1500921.
- 591 21. Goulart CP, Mahmudi M, Crona KA, Jacobs SD, Kallmann M, Hall BG,
- 592 Greene DC, Barlow M. 2013. Designing antibiotic cycling strategies by
 593 determining and understanding local adaptive landscapes. PLoS ONE 8:e56040.
- 594 22. Ogbunugafor CB, Wylie CS, Diakite I, Weinreich DM, Hartl DL. 2016.
 595 Adaptive landscape by environment interactions dictate evolutionary dynamics in
- 596 models of drug resistance. PLoS Comput Biol **12**:e1004710.
- 597 23. Schenk MF, Witte S, Salverda MLM, Koopmanschap B, Krug J, de Visser
- JAGM. 2015. Role of pleiotropy during adaptation of TEM-1 β-lactamase to two
 novel antibiotics. Evol Appl 8:248-260.
- 600 24. Flynn KM, Cooper TF, Moore FBG, Cooper VS. 2013. The environment affects
 601 epistatic interactions to alter the topology of an empirical fitness landscape. PLoS
 602 Genet 9:e1003426.

- 603 25. Agudelo-Romero P, Carbonell P, Pérez-Amador MA, Elena SF. 2008. Virus
- adaptation by manipulation of host's gene expression. PLoS ONE **3**:e2397.
- 26. Lalić J, Elena SF. 2015. The impact of high-order epistasis in the within-host
 fitness of a positive-sense plant RNA virus. J Evol Biol 28:2236-2247.
- 607 27. Bedoya L, Daròs JA. 2010. Stability of *Tobacco etch virus* infectious clones in
 608 plasmid vectors. Virus Res 149:234-240.
- 609 28. Carrasco P, de la Iglesia F, Elena SF. 2007. Distribution of fitness and virulence
- effects caused by single-nucleotide substitutions in *Tobacco etch virus*. J Virol
 81:12979-12984.
- 612 29. Boyes DC, Zayed AM, Ascenzi R, McCaskill MJ, Hoffman NE, Davis KR,
 613 Görlach J. 2001. Growth stage-based phenotypic analysis of *Arabidopsis*: a model
- 614 for high throughput functional genomics in plants. Plant Cell **13**:1499-1510.
- 615 30. Lalić J, Agudelo-Romero P, Carrasco P, Elena SF. 2010. Adaptation of tobacco
- 616 etch potyvirus to a susceptible ecotype of Arabidopsis thaliana capacitates it for
- 617 systemic infection of resistant ecotypes. Phil Trans R Soc B 65:1997-2008.
- 618 31. Aita T, Iwakura M, Husimi Y. 2001. A cross-section of the fitness landscape of
 619 dihydrofolate reductase. Protein Eng 14:633-638.
- 620 32. Ferreti L, Schmiegelt B, Weinreich DM, Yamauchi A, Kobayashi Y, Tajima F,
- Achaz G. 2016. Measuring epistasis in fitness landscapes: the correlation of fitness
 effects of mutations. J Theor Biol 396:132-143.
- 33. Brouillet S, Annoni H, Ferreti L, Achaz G. 2016. MAGELLAN: a tool to explore
 small fitness landscapes. bioRxiv 031583.
- 625 34. Kouyos RD, Silander OK, Bonhoeffer S. 2007. Epistasis between deleterious
- 626 mutations and the evolution of recombination. Trends Ecol Evol **22**:308-315.

- 627 35. Gao H, Granka JM, Feldman MW. 2010. On the classification of epistatic
 628 interactions. Genetics 184:827-837.
- 629 36. Poelwijk FJ, Tanase-Nicola S, Kiviet DJ, Tans SJ. 2011. Reciprocal sign
 630 epistasis is a necessary condition for multi-peaked fitness landscapes. J Theor Biol
 631 272:141-144.
- 632 37. Weinreich DM, Lan Y, Wylie CS, Heckendorn RB. 2013. Should evolutionary
 633 geneticists worry about higher-order epistasis? Curr Opin Genet Develop 23:700634 707.
- 635 38. Cui H, Wang A. 2016. *Plum pox virus* 6K1 protein is required for viral replication
 636 and targets the viral replication complex at the early stage of infection. J Virol
 637 90:5119-5131.
- 638 39. Elena SF, Rodrigo G. 2012. Towards an integrated molecular model of plant-virus
 639 interactions. Curr Opin Virol 2:719-724.
- 40. Martin G, Elena SF, Lenormand T. 2007. Distribution of epistasis in microbes fit
 predictions from a fitness landscape model. Nat Genet 39:555-560.
- 642 41. Kingman J. 1987. A simple model for the balance between selection and mutation.
 643 J Appl Probab 15:1-12.
- 42. Aita T, Uchiyama H, Inaoka T, Nakajima M, Kokubo T, Husimi Y. 2000.
 Analysis of a local fitness landscape with a model of the rough Mt. Fuji-type
 landscape: application to prolyl endopeptidase and thermolysis. Biopolymers
 54:64-79.
- 648 43. Bedhomme S, Hillung J, Elena SF. 2015. Emerging viruses: why they are not
 649 jacks of all trades? Curr Opin Virol 10:1-6.
- 44. Fry JD. 1996. The evolution of host specialization: are trade-offs overrated? Am
 Nat 148:S84-S107.

- 45. Smith-Tsurkan SD, Wilke CO, Novella IS. 2010. Incongruent fitness landscapes,
- not tradeoffs, dominate the adaptation of *Vesicular stomatitis virus* to novel host
 types, J Gen Virol 91:1484-1493.
- 654 types. J Gen Virol **91**:1484-1493.
- 655 46. Da Silva J. 2009. An adaptive walk by *Human immunodeficiency virus* type 1
- through a fluctuation fitness landscape. Evolution **64**:1160-1165.
- 47. Da Silva J, Coetzer M, Nedellec R, Pastore C, Mosier DE. 2010. Fitness
 epistasis and constraints on adaptation in a *Human immunodeficiency virus* type 1
- protein region. Genetics **185**:293-303.
- 48. Da Silva J, Wyatt SK. 2014. Fitness valleys constrain HIV-1's adaptation to its
 secondary chemokine coreceptor. J Evol Biol 27:604-615.
- 662 49. Kouyos RD, Leventhal GE, Hinkley T, Haddad M, Whitcomb JM,
- 663 Petropoulos CJ, Bonhoeffer S. 2012. Exploring the complexity of the HIV-1
 664 fitness landscape. PLoS Genet 8:e1002551.
- 50. Proulx SR. 2011. The rate of multi-step evolution in Moran and Wright-Fisher
 populations. Theor Pop Biol 80:197-207.
- 51. Tromas N, Zwart MP, Poulain M, Elena SF. 2014. Estimation of the *in vivo*recombination rate for a plant RNA virus. J Gen Virol 95:724-732.
- 669 52. Simon-Loriere E, Holmes EC. 2011. Why do RNA viruses recombine? Nat Rev
- 670 Microbiol **9:**617-626.
- 53. Sanjuán R, Nebot MR, Chirico N, Mansky LM, Belshaw R. 2010. Viral
 mutation rates. J Virol 19:9733-9748.
- 673 54. Tromas N, Elena SF. 2010. The rate and spectrum of spontaneous mutations in a
- 674 plant RNA virus. Genetics **185**:983-989.

675 55. Hillung J, Cuevas JM, Elena SF. 2012. Transcript profiling of different 676 Arabidopsis thaliana ecotypes in response to tobacco etch potyvirus infection. Front Microbiol 3:229. 677 678 56. Hillung J, Cuevas JM, Valverde S, Elena SF. 2014. Experimental evolution of an 679 emerging plant virus in host genotypes that differ in their susceptibility to infection. 680 Evolution 68:2467-2480. 681 57. Hillung J, Cuevas JM, Elena SF. 2015. Evaluating the within-host fitness effects 682 of mutations fixed during virus adaptation to different ecotypes of a new host. Phil 683 Trans R Soc B 370:20140292. 684 58. Hillung J, García-García F, Dopazo J, Cuevas JM, Elena SF. 2016. The 685 transcriptomics of an experimentally evolved plant-virus interaction. Sci Rep 686 **6:**24901. 687 59. Cervera H, Lalić J, Elena SF. 2016. Efficient escape from local optima in a 688 highly rugged fitness landscape by evolving RNA virus populations. Proc R Soc B 689 283:20160984. 690 60. Pagán I, Alonso-Blanco C, García-Arenal F. 2008. Host responses in life-history 691 traits and tolerance to virus infection in Arabidopsis thaliana. PLoS Pathog

- 692 **4:**e1000124.
- 693

694

TABLE 1 Set of mutations included in this study.

| Label | Mutation | Gene | Amino acid change ^a |
|-------|----------|-----------|--------------------------------|
| 00000 | U357C | P1 | synonymous |
| 0000 | C3140U | <i>P3</i> | A999V |
| 00000 | C3629U | 6K1 | T1162M |
| 00000 | C6037U | VPg | L1965F |
| 0000● | C6906U | NIaPro | synonymous |

^a Numeration according to the amino acid residue in the polyprotein.

 \sum

Journal of Virology

696

Statistics^a A. thaliana N. tabacum General: Peaks 2 4 Sinks 0 0 Epistasis: 1.902 1.697 Mean slope to roughness ratio (θ) Correlation between neighbors' 0.119 0.111 fitness (ρ) Frequency multiplicative 0.013 0.013 Frequency magnitude 0.662 0.575 0.188 Frequency sign 0.212 Frequency reciprocal sign 0.113 0.225

TABLE 2Summary statistics describing the topography of bothlandscapes.

^a Computed using the MAGELLAN webserver (33).

697

Journal of Virology

| Factor | LRT ^a | df | Р | η_P^2 b | $1 - \beta^{c}$ |
|-----------|------------------|-----|---------|--------------|-----------------|
| Intercept | 3979.285 | 1 | < 0.001 | 0.982 | 1 |
| G | 2397.695 | 31 | < 0.001 | 0.860 | 1 |
| Н | 4.341 | 1 | 0.037 | 0.006 | 0.183 |
| GxH | 1344.481 | 20 | < 0.001 | 0.500 | 1 |
| P(GxH) | 1168.930 | 177 | < 0.001 | 0.848 | 1 |

^a Likelihood ratio test.

^b Magnitude of effects associated to each model factor.

^c Statistical power of the corresponding tests.

698

| | A. thaliana | | | | | |
|-----------------|-------------|-----------|------|-----------------|--|--|
| N. tabacum | No | Magnitude | Sign | Reciprocal sign | | |
| No | 37 | 8 | 1 | 0 | | |
| Magnitude | 2 | 9 | 0 | 0 | | |
| Sign | 1 | 4 | 0 | 2 | | |
| Reciprocal sign | 0 | 5 | 3 | 3 | | |

TABLE 4 Epistasis transition matrix.

699

 \leq

700 FIG 1 Different types of epistasis between two loci defining the fitness of a genotype. 701 Small letters indicate the wildtype and capital letters the mutant alleles. (a) In case of 702 no epistasis, the fitness of the double mutant ●● results from multiplying the fitness 703 effects of both mutations on the wildtype genetic background (i.e., the fitnesses of 704 genotypes $\bullet \circ$ and $\circ \bullet$). (b) If magnitude epistasis exists, the fitness of the double 705 mutant $\bullet \bullet is$ different from the multiplicative expectation. In the example, the 706 observed fitness of $\bullet \bullet$ is larger than expected as a consequence of positive epistasis. 707 Both in the cases of no epistasis or of magnitude epistasis, the effects of mutations $\bullet \bigcirc$ 708 and $\bigcirc \bullet$ are unconditionally beneficial. (c) If the effect of one of the mutations is 709 conditionally beneficial (i.e., beneficial in one genetic background but deleterious in 710 another), then we are in the situation of sign epistasis. (d) Finally, if both mutations $\bullet \bigcirc$ 711 and $\bigcirc \bullet$ are deleterious by themselves, but beneficial when combined, we are in the 712 situation of reciprocal sign epistasis.

713

714 FIG 2 Empirical fitness landscapes evaluated for the set of five mutations fixed by TEV 715 during its experimental adaptation to A. thaliana. The fitness of the 32 genotypes was 716 evaluated in the novel host (a) and in the original one, N. tabacum (b). Each string of 717 dots represents a genotype. Black dots represent a mutation in the corresponding locus, 718 while white dots correspond to the wildtype allele on this locus. Genotypes in a green 719 box correspond to local fitness peaks. Green lines correspond to beneficial mutations, 720 red lines to deleterious mutations and orange lines to neutral changes (in the direction 721 from genotype $\bigcirc \bigcirc \bigcirc \bigcirc \bigcirc \bigcirc$ to genotype $\bigcirc \bigcirc \bigcirc \bigcirc \bigcirc$). Graphs generated with the 722 MAGELLAN webserver (33).

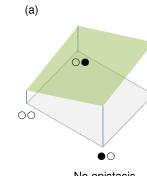
723

| 724 | FIG 3 Fitness values and epistasis coefficients in both hosts. (a) Fitness values |
|-----|---|
| 725 | estimated for the 32 genotypes shown in Fig. 2 in both hosts. In both hosts, fitness is |
| 726 | expressed relative to the wildtype genotype 00000. Dashed lines correspond to the |
| 727 | fitness of wildtype on each host. The $(0, 0)$ dot correspond includes the nine cases of |
| 728 | unconditionally lethal genotypes. (b) Distribution of epistasis on both hosts. Dashed |
| 729 | lines correspond to the case of multiplicative fitness effects (no epistasis). Error bars |
| 730 | correspond to ± 1 SD. |

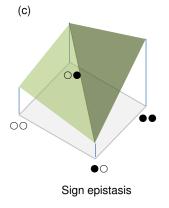
731

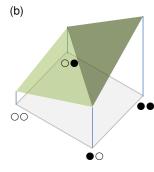
FIG 4 The Walsh's coefficient of order zero is the mean fitness across all genotypes; fitness values were normalized to make this figure equal to one. First-order and secondorder coefficients are analogous to selection coefficients and pairwise epistasis, respectively. Higher order terms are equivalent to epistasis among increasing numbers of mutations. Walsh's coefficients were computed with the MAGELLAN webserver (33).

Journal of Virology



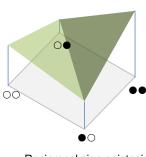






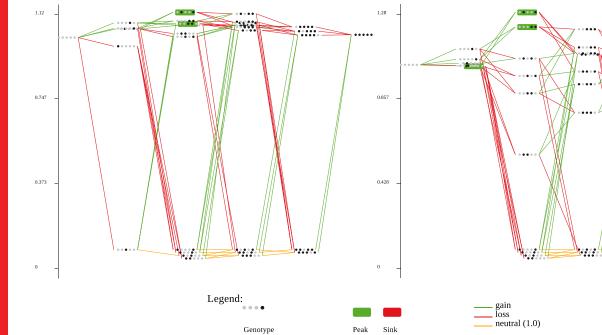
Magnitude epistasis

(d)



Reciprocal sign epistasis

 \leq

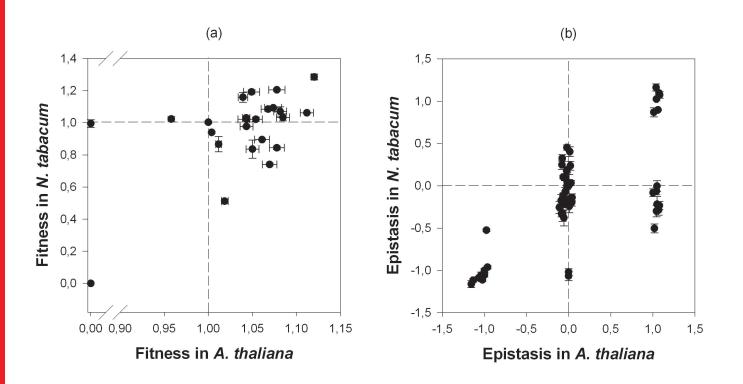


(a)

(b)

 $\overline{\leq}$

Journal of Virology



 \leq



